Supporting Information for

# Circularly Polarized Near-Infrared Phosphorescence of Chiral Chromium(III) Complexes

Yang Cheng,[a] Jiang He,[a] Wenjie Zou,[a] Xiaoyong Chang,[a] Qingqing Yang,*[a] and Wei Lu*[a]

[a]Department of Chemistry, Southern University of Science and Technology, Shenzhen, Guangdong 518055, P. R. China.

E-mail: yangqq3@sustech.edu.cn;

luw@sustech.edu.cn.

## 1. Materials and Methods

Complexes **1**–**3** were prepared according to the literature methods.[1] All other reagents were commercially available. Complexes used for test were purified by column chromatography and recrystallized by slow diffusion of petroleum ether into dichloromethane solutions to yield the complexes as crystalline solids. NMR spectra were recorded with a Bruker Avance DPX 400 MHz and 500 MHz instrument. HRMS (ESI) spectra were obtained using a Thermo Fisher Q-Exactive Mass Spectrometer. UV-Vis absorption measurements were recorded using a Thermo Scientific Evolution 201 UV-Visible Spectrophotometer. The EPR experiments were carried out on the Bruker E500 variable temperature magnetic resonance instrument at 100 K. X-ray photoelectron spectroscopy (XPS) and ultraviolet photoelectron spectroscopy (UPS) spectra were recorded using a ULVAC PHI 5000 VersaProbe III system equipped with an Al Kα X-ray source. CV experiments were performed on a one-compartment three electrode cell in MeCN with 0.1 M $^{n}Bu_4NPF_6$ by using CHI-620E in glovebox. Glassy carbon disk electrodes were used as working, platinum wire as auxiliary and Ag/AgCl or Ag as reference electrode. All potentials reported herein were converted to their corresponding values versus $Fc^{0/+}$. The ferrocene was added after test. Spectro-electrochemical experiments were performed in Thermo Scientific Evolution 201 UV-Visible spectrophotometer in combination with a home-built sample compartment consisting of a quartzose cell with an open window and an adjustable three electrodes (indium tin oxide (ITO) glass substrates as working electrode, 1 mm platinum counter and Ag/AgCl reference electrode). The added bias was controlled by the constant-potential electrolysis mode for 500 s. Emission spectra and lifetime measurements were acquired via Edinburg spectrometer FLS-980 equipped with MCP-PMT and NIR-PMT detectors. Absolute luminescent quantum yields were recorded with Hamamatsu absolute PL quantum yield spectrometer C11347. Time-resolved transient absorption spectra were performed with Edinburgh LP-920 Laser Flash Photolysis Spectrometer equipped with ICCD detector. Circular dichroism (CD) and circularly polarized luminescence (CPL) were performed via Applied Photophysics Chirascan circular dichroism spectrometers and JASCO CPL-300, respectively.

## 2. Synthesis of complexes 1–3

Preparation of ligands **L1**–**L3**

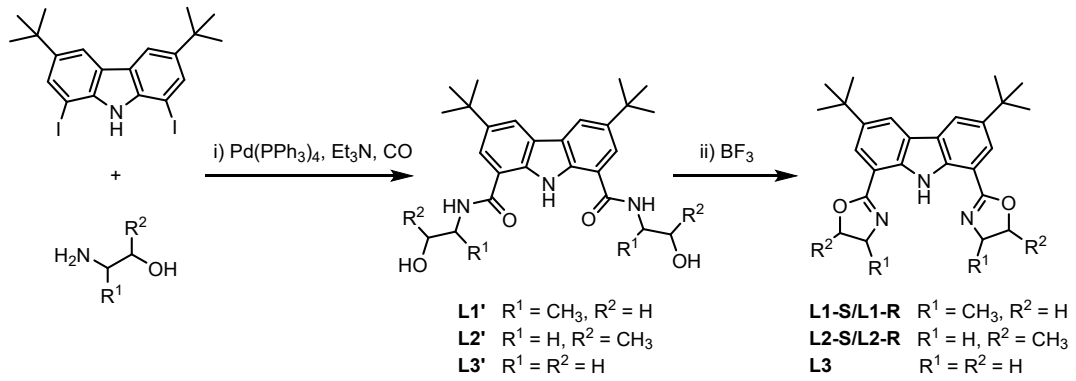


A modified procedure reported was used for **L1**–**L3**.[2] After obtaining the desired 1,8-dihalo precursors, we carried out Pd-catalyzed carbonylative amidation with amino alcohols derived by reduction of the corresponding chiral amino acids. The amino alcohols ((R/S)-(±)-2-Amino-1-propanol, 5 mmol, 375 mg ), 3,6-Bis(1,1-dimethylethyl)-1,8-diiodo-carbazole (1 mmol, 531 mg), $Pd(PPh_3)_4$ (20 mol %) and $Et_3N$ (1.2 mL) were added into 8 m L of dry, degassed DMF via a syringe. The reaction mixture was stirred at 60˚C for 8 h under a CO atmosphere. After the mixture was cooled down, it was diluted with $CH_2Cl_2$ and washed with brine and 1 M $CuSO_4$ for 3 times. The organic phase was dried over $Na_2SO_4$ and concentrated under reduced pressure to give the **L1'**. **L1'** was partially purified by passing through a short kieselguhr bed and eluting with methanol. The eluent was concentrated under rotovap, dried under vacuum. Then **L1'** was suspended in 15% w/v of $BF_3$•$Et_2O$. The suspension liquid was stirred at 120 ˚C for 6 h. The reaction mixture was cooled to room temperature and poured into ice cold 2 M NaOH (10 m L), extracted with $CH_2Cl_2$ and washed with a saturated $NaHCO_3$, dried over $Na_2SO_4$, concentrated under reduced pressure. The residue was purified by silica gel chromatography ($CH_2Cl_2$) to afford 31% of the product **L1** as a yellow solid. **L2** and **L3** were prepared in the same way.

**L1-R** $^1$H NMR (400 MHz, $CDCl_3$): $\delta$ 11.59 (s, 1H), 8.25 (d, $J$ = 1.8 Hz, 2H), 8.00 (d, $J$ = 1.7 Hz, 2H), 4.66 – 4.49 (m, 4H), 4.02 (t, $J$ = 7.4 Hz, 2H), 1.50 – 1.49 (m, 24 H) ppm. $^{13}$C{$^1$H} NMR (126 MHz, $CDCl_3$): $\delta$ 163.11, 141.75, 137.64, 123.52, 123.35, 119.97, 109.72, 73.61, 62.24, 34.92, 32.15, 21.84 ppm.

**L1-S** $^1$H NMR (400 MHz, $CDCl_3$): $\delta$ 11.61 (s, 1H), 8.26 (d, $J$ = 1.7 Hz, 2H), 8.01 (d, $J$ = 1.7 Hz, 2H), 4.67 – 4.50 (m, 4H), 4.02 (t, $J$ = 7.3 Hz, 2H), 1.50 – 1.49 (m, 24H) ppm. $^{13}$C{$^1$H} NMR (126 MHz, $CDCl_3$): $\delta$ 163.08, 141.73, 137.64, 123.52, 123.32, 119.94, 109.74, 73.59, 62.25, 34.91, 32.14, 21.84 ppm.

**L2-R** $^1$H NMR (400 MHz, $CDCl_3$): $\delta$ 11.48 (s, 1H), 8.24 (d, $J$ = 1.6 Hz, 2H), 8.02 (s, 2H), 4.98 – 4.89 (m, 2H), 4.33 (dd, $J$ = 14.2, 9.3 Hz, 2H), 3.80 (dd, $J$ = 14.2, 7.4 Hz, 2H), 1.52 (d, $J$ = 6.2 Hz, 6H), 1.49 (s, 18H) ppm. $^{13}$C{$^1$H} NMR (126 MHz, $CDCl_3$): $\delta$ 163.98, 141.88, 137.57, 123.61, 123.58, 120.15, 109.73, 75.99, 61.52, 34.96, 32.16, 21.31 ppm.

**L2-S** $^{1}$H NMR (400 MHz, $CDCl_3$): $\delta$ 11.49 (s, 1H), 8.24 (d, $J$ = 1.7 Hz, 2H), 8.01 (s, 2H), 4.99 – 4.87 (m, 2H), 4.33 (dd, $J$ = 14.2, 9.3 Hz, 2H), 3.80 (dd, $J$ = 14.2, 7.4 Hz, 2H), 1.52 (d, $J$ = 6.2 Hz, 6H), 1.49 (s, 18H) ppm. $^{13}$C{$^{1}$H} NMR (126 MHz, $CDCl_3$): $\delta$ 163.87, 141.81, 137.57, 123.56, 123.52, 120.03, 109.86, 75.87, 61.69, 34.95, 32.16, 21.32 ppm.

**L3** $^{1}$H NMR (500 MHz, $CDCl_3$): $\delta$ 11.54 (s, 1H), 8.30 (d, $J$ = 1.7 Hz, 2H), 8.04 (d, $J$ = 1.8 Hz, 2H), 4.48 (t, $J$ = 9.4 Hz, 4H), 4.25 (t, $J$ = 9.4 Hz, 4H), 1.52 (s, 18H) ppm. $^{13}$C{$^{1}$H} NMR (126 MHz, $CDCl_3$): $\delta$ 164.21, 141.77, 137.49, 123.54, 123.45, 119.92, 109.71, 67.01, 55.21, 34.87, 32.10 ppm.

**General Procedure**: Synthesis of Cr(III) complexes

Under a nitrogen atmosphere, the ligand (0.5 mmol, 1.0 equiv.) was dissolved in dry tetrahydrofuran (10 mL) and the mixture was cooled to −78 °C. Lithium diisopropylamide (0.28 mL, 2.0 M, 1.1 equiv.) was added drop-wise and the reaction mixture was stirred for 30 min at −78 °C. The resulted solution was allowed to warm to room temperature and stirred for 2 h. A suspension of $CrCl_2$ (36.8 mg, 0.3 mmol, 0.6 equiv.) in dry tetrahydrofuran (10 mL) was then added drop-wise. The luminous yellow reaction mixture was stirred at room temperature for 48 h under the nitrogen atmosphere. The dark-red reaction mixture was then stirred under air for 30 min before work-up. The solvent was removed in vacuo and the residue was dissolved in methanol (5 mL) which was then added drop-wise into a solution of an aqueous solution of $NH_4PF_6$ (2 M, 50 mL). The resulting precipitate was filtered off, washed with water for three times and then dissolved in dichloromethane. The solution was dried over $Na_2SO_4$ and concentrated under reduced pressure. The residue was purified by flash chromatography on silica gel (eluent: $CH_2Cl_2$/MeOH, v/v = 100/1) and recrystallized by slow diffusion of petroleum ether into dichloromethane solutions to yield the Cr(III) complexes as crystalline solids.

**1R:** Following the general procedure, **1R** was isolated as a dark orange crystals (29 mg, 11% yield). Anal. Calcd for $C_{56}H_{68}CrF_6N_6O_4P$: C, 61.93; H, 6.31; N, 7.74; Found: C, 61.66; H, 6.37; N, 7.61. HR-MS: *m/z* 940.4694 (calculated for $[M]^+$ 940.4702).

**1S:** Following the general procedure, **1S** was isolated as a dark orange crystals (26 mg, 10% yield). Anal. Calcd for $C_{56}H_{68}CrF_6N_6O_4P$: C, 61.93; H, 6.31; N, 7.74; Found: C, 61.65; H, 6.40; N, 7.66. HR-MS: *m/z* 940.4691 (calculated for $[M]^+$ 940.4702).

**2R:** Following the general procedure, **2R** was isolated as orange crystals (37 mg, 14% yield). Anal. Calcd for $C_{56}H_{68}CrF_6N_6O_4P$: C, 61.93; H, 6.31; N, 7.74; Found: C, 61.97; H, 6.58; N, 7.34. HR-MS: *m/z* 940.4695 (calculated for $[M]^+$ 940.4702).

**2S:** Following the general procedure, **2S** was isolated as orange crystals (28 mg, 10% yield). Anal. Calcd for $C_{56}H_{68}CrF_6N_6O_4P$: C, 61.93; H, 6.31; N, 7.74; Found: C, 61.58; H, 6.35; N, 7.50. HR-MS: *m/z* 940.4690 (calculated for $[M]^+$ 940.4702).

**3:** Following the general procedure, **3** was isolated as orange crystals (21 mg, 8% yield). Anal. Calcd for $C_{52}H_{60}CrF_6N_6O_4P$: C, 60.64; H, 5.87; N, 8.16; Found: C, 60.28; H, 5.95; N, 8.10. HR-MS: MS: *m/z* 884.4067 (calculated for $[M]^+$ 884.4076).

## 3. NMR spectroscopy

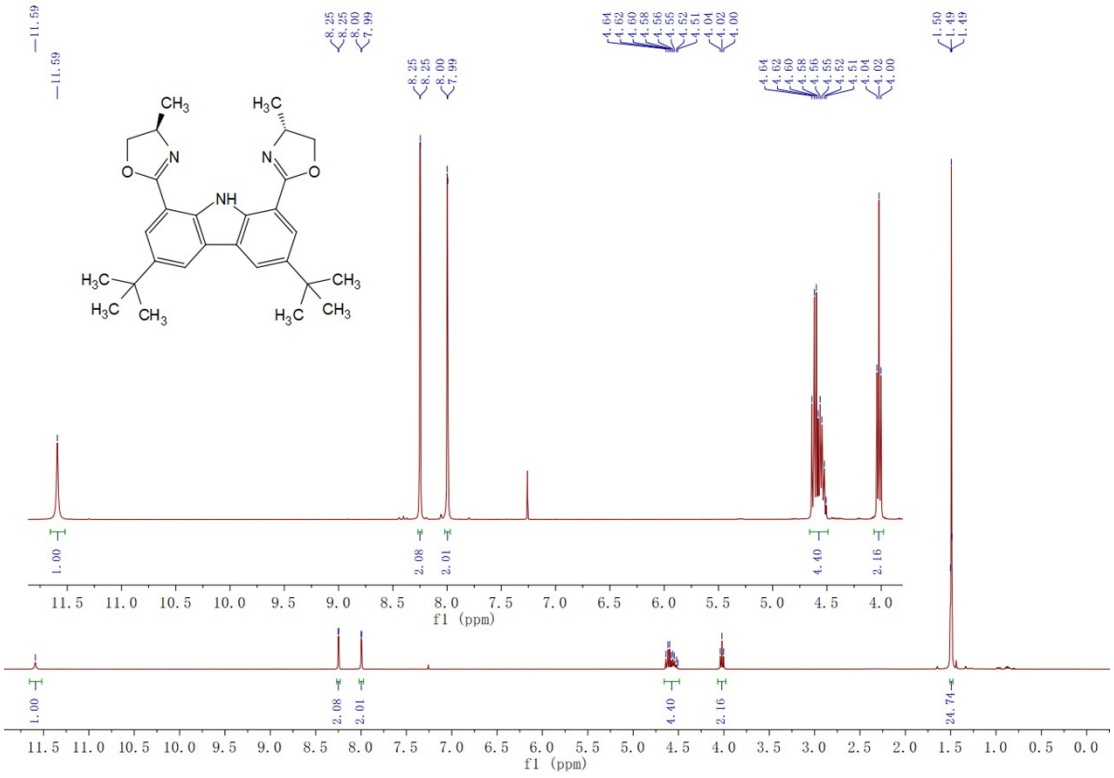


**Figure S1**. $^1$H NMR spectrum of **L1-R** (400 MHz, $CDCl_3$).

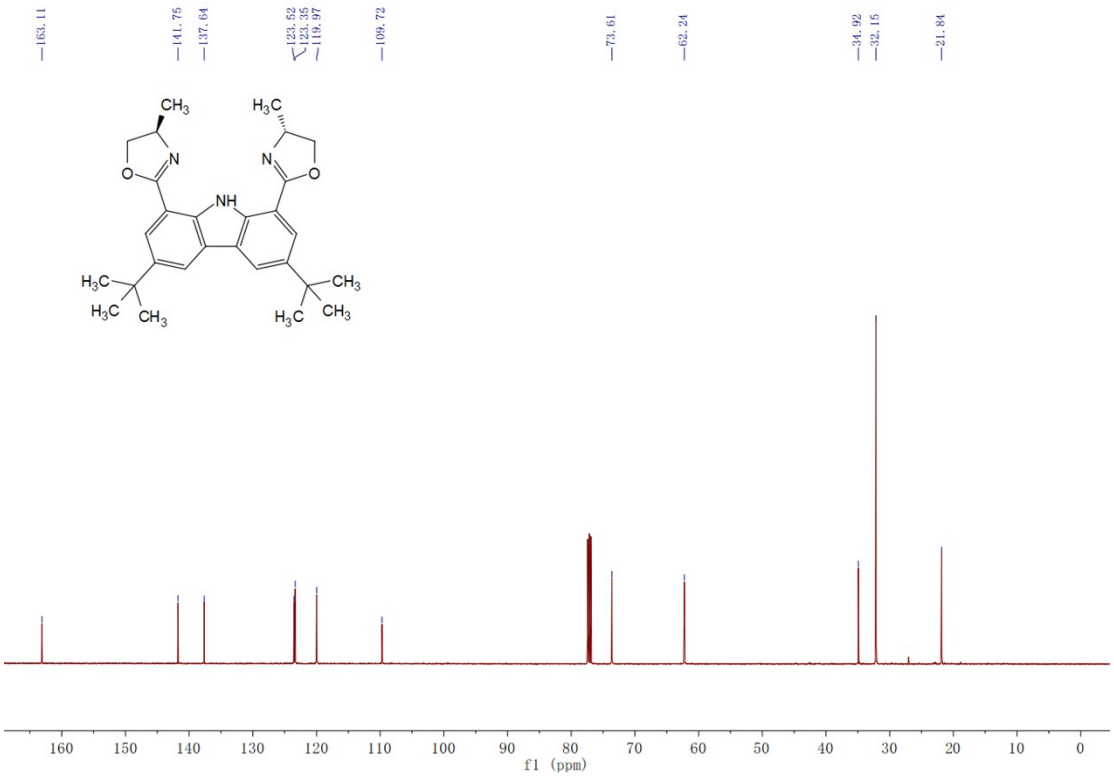


**Figure S2**. $^{13}C\{^{1}H\}$ NMR spectrum of **L1-R** (126 MHz, $CDCl_3$).

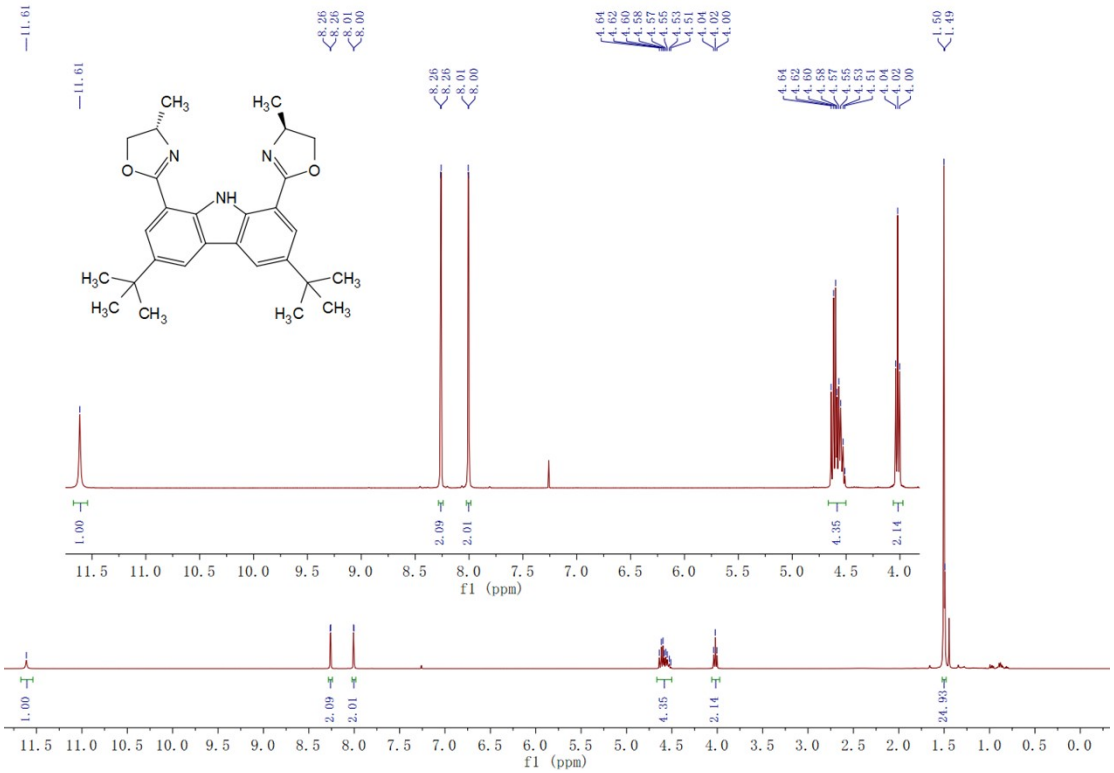


**Figure S3**. $^{1}H$ NMR spectrum of **L1-S** (400 MHz, $CDCl_3$).

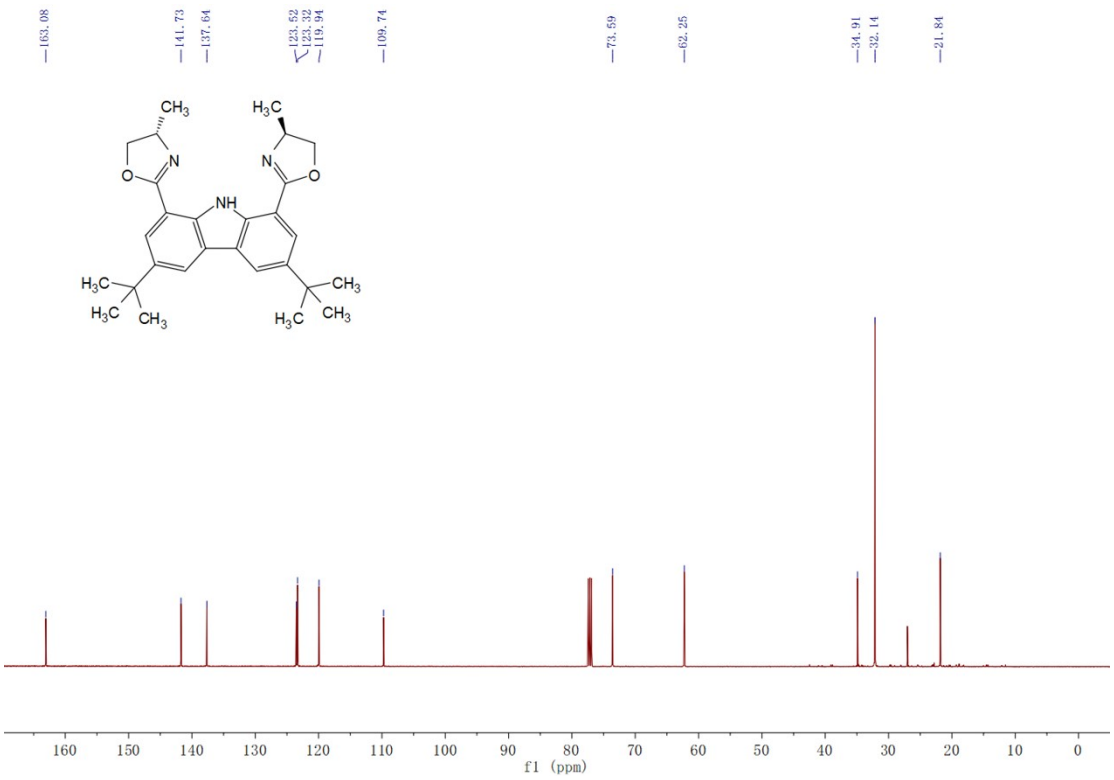


**Figure S4**. $^{13}C\{^{1}H\}$ NMR spectrum of **L1-S** (126 MHz, $CDCl_3$).

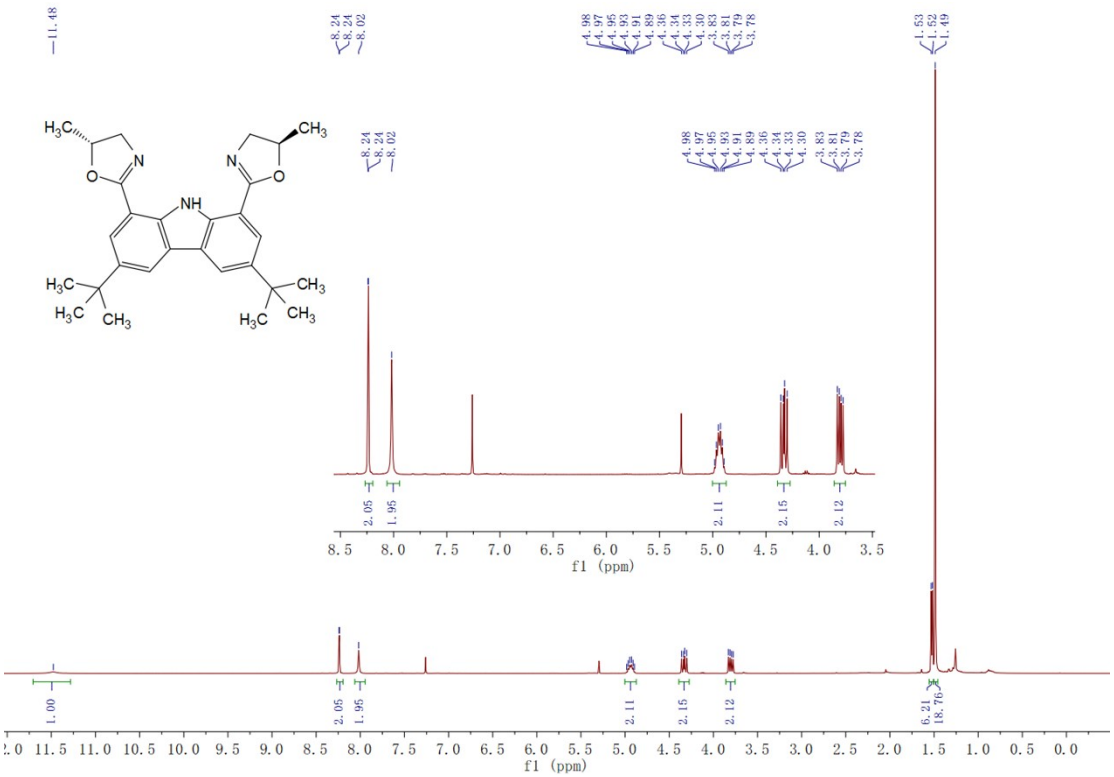


**Figure S5**. $^{1}H$ NMR spectrum of **L2-R** (400 MHz, $CDCl_3$).

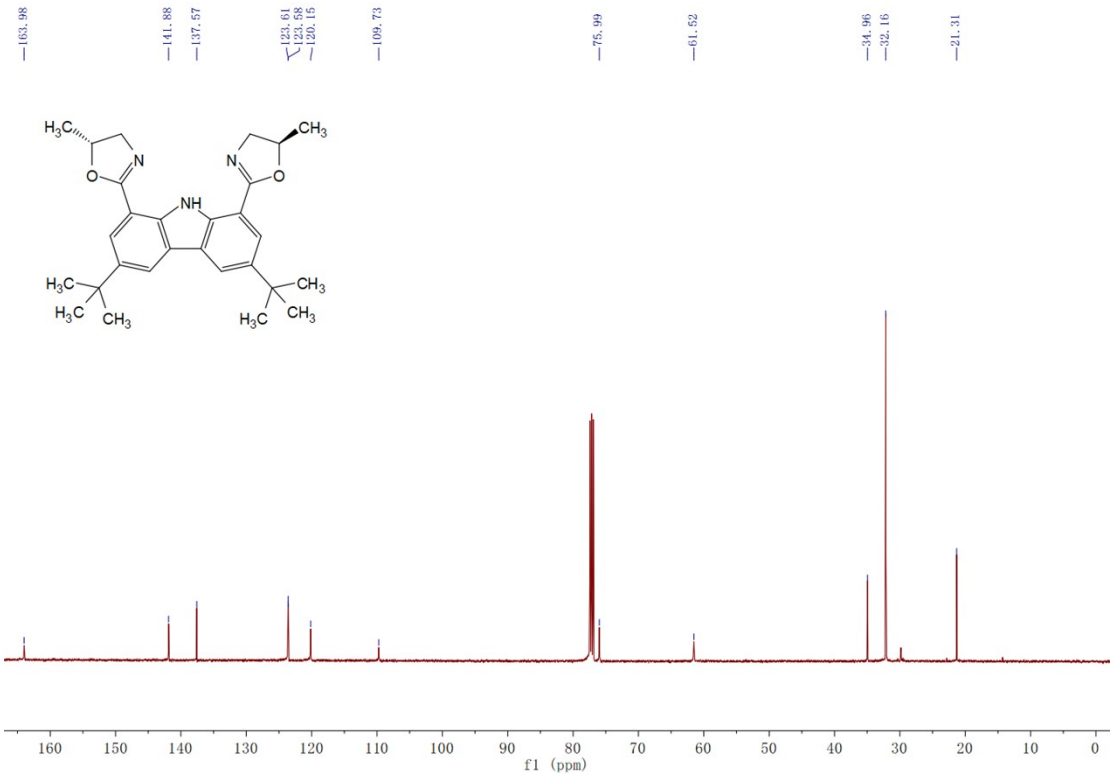


**Figure S6**. $^{13}C\{^{1}H\}$ NMR spectrum of **L2-R** (126 MHz, $CDCl_3$).

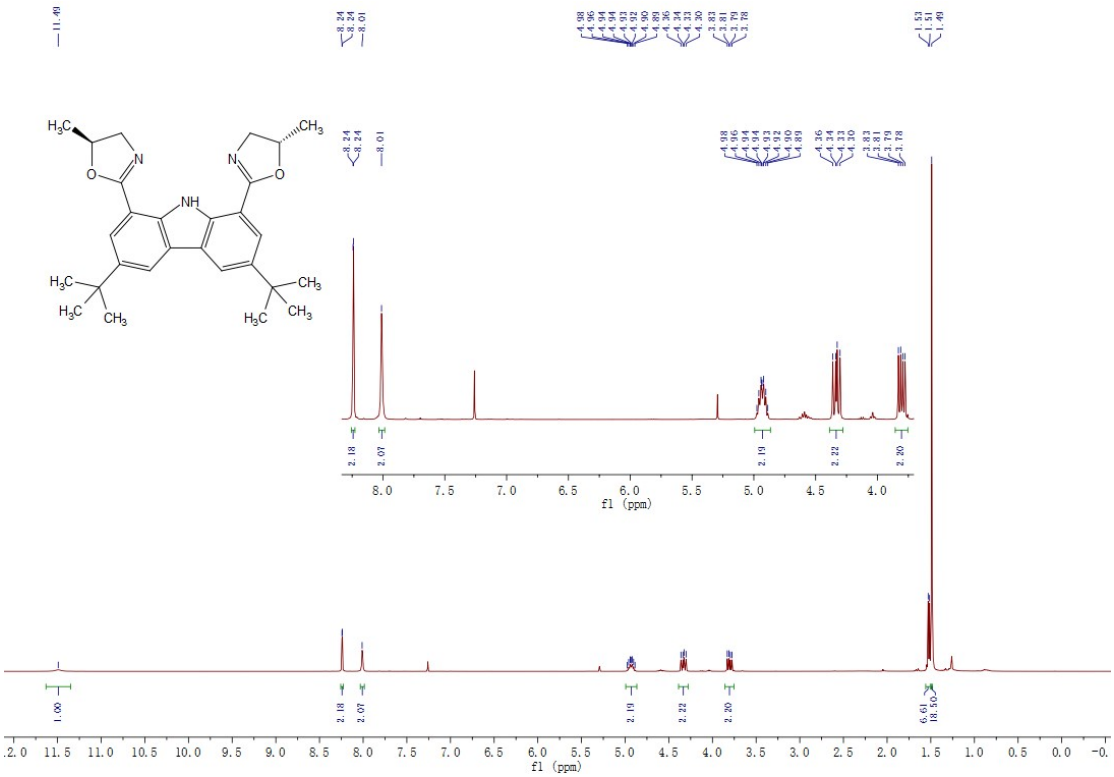


**Figure S7**. $^{1}H$ NMR spectrum of **L2-S** (400 MHz, $CDCl_3$).

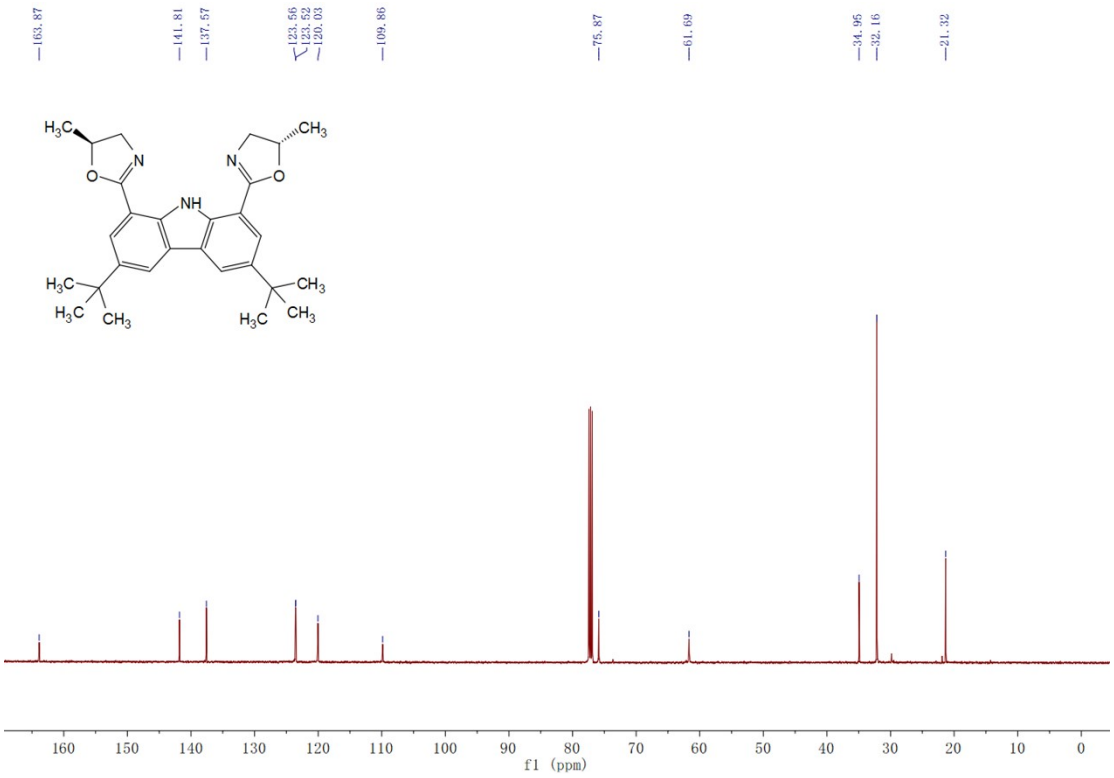


**Figure S8**. $^{13}C\{^{1}H\}$ NMR spectrum of **L2-S** (126 MHz, $CDCl_3$).

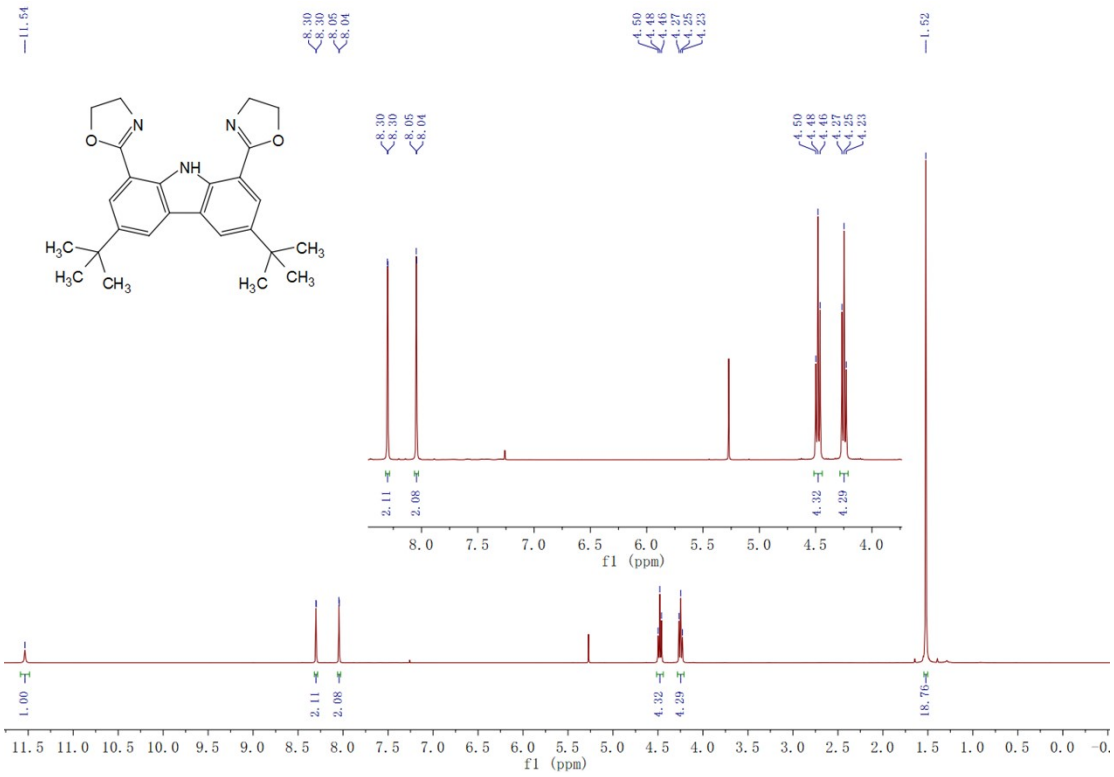


**Figure S9**. $^{1}H$ NMR spectrum of **L3** (500 MHz, $CDCl_3$).

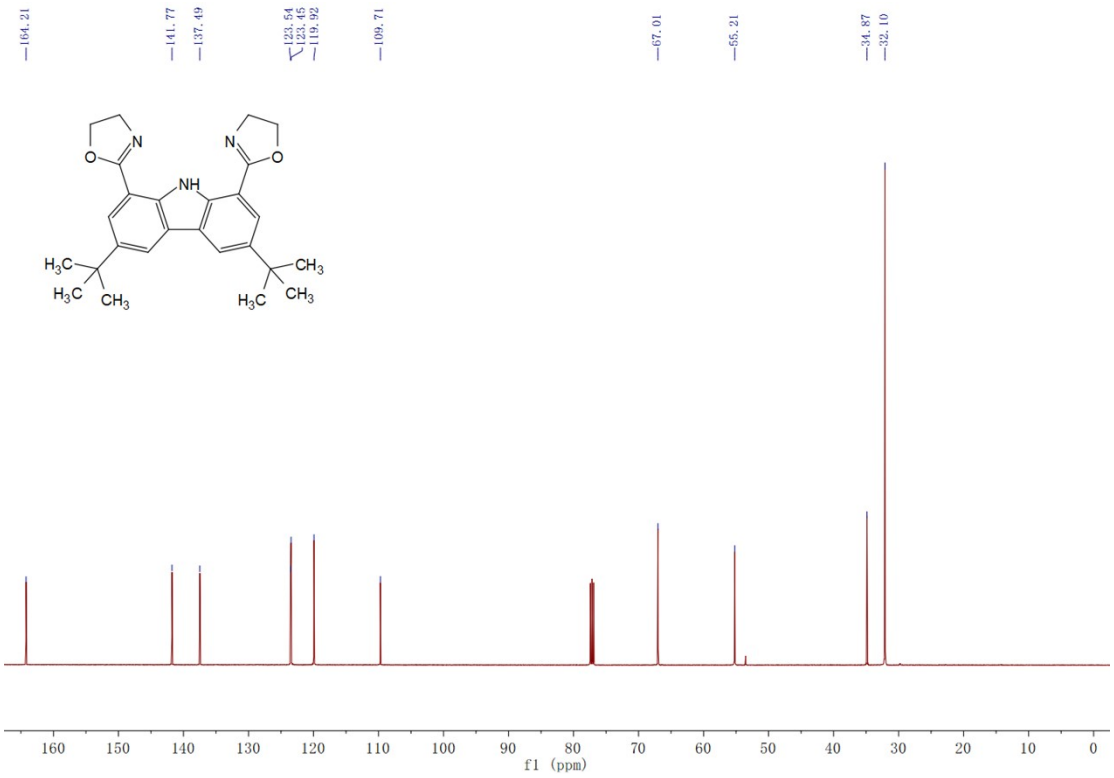


**Figure S10**. $^{13}C\{^{1}H\}$ NMR spectrum of **L3** (126 MHz, $CDCl_3$).

## 4. Mass spectra

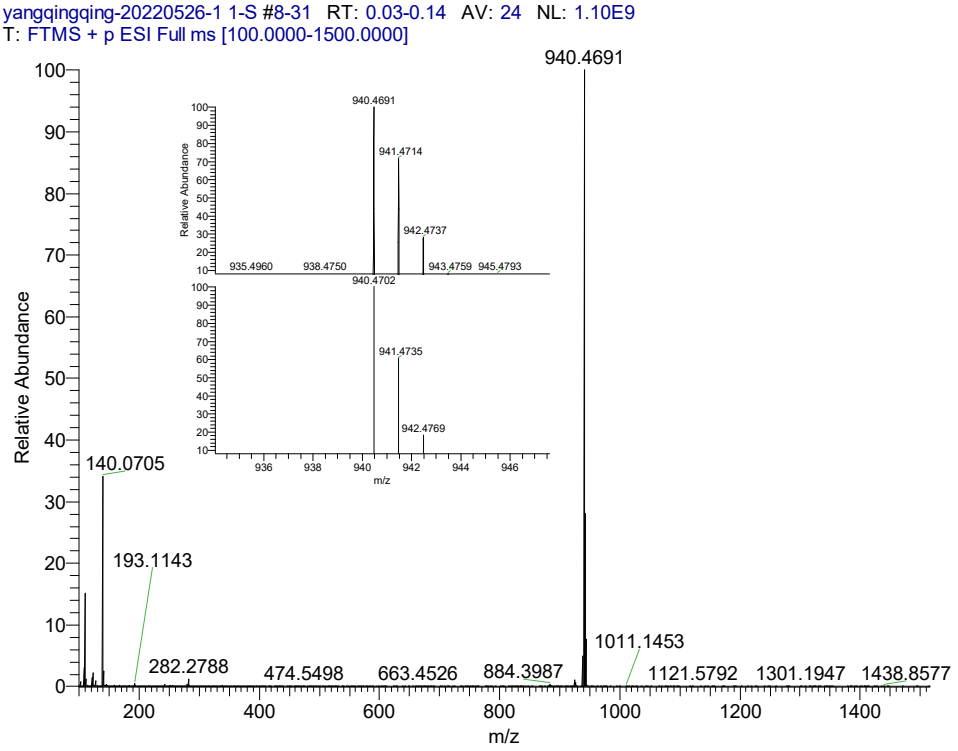


**Figure S11**. HR-MS (ESI) mass spectrum of **1S**. The insets depict the experimental (top) and calculated (bottom) isotopic pattern of the peak.

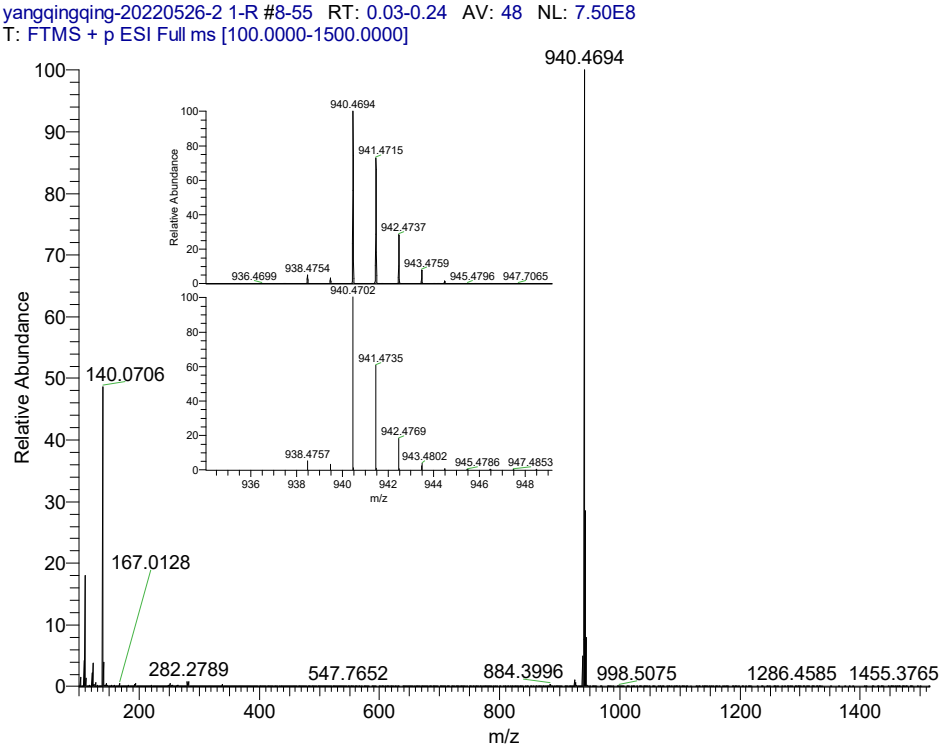


**Figure S12**. HR-MS (ESI) mass spectrum of **1R**. The insets depict the experimental (top) and calculated (bottom) isotopic pattern of the peak.

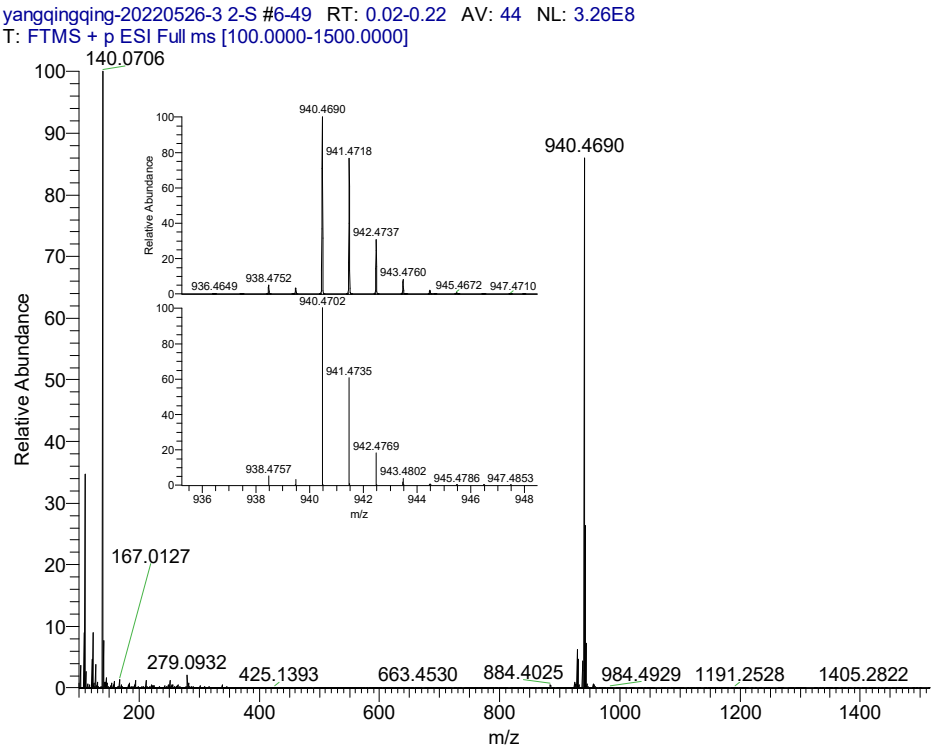


**Figure S13**. HR-MS (ESI) mass spectrum of **2S**. The insets depict the experimental (top) and calculated (bottom) isotopic pattern of the peak.

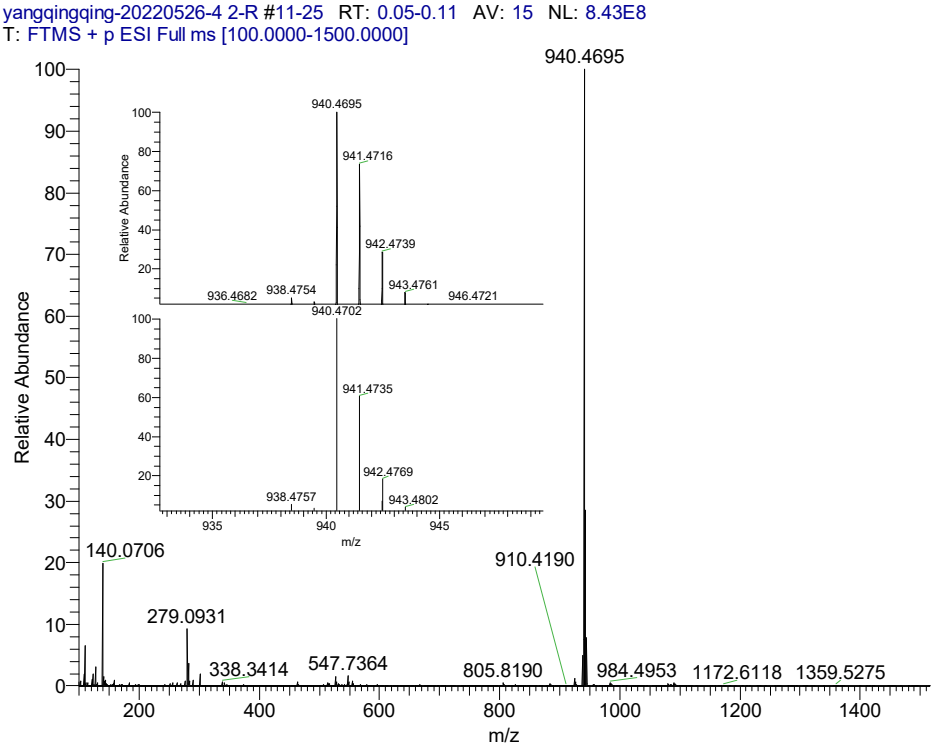


**Figure S14**. HR-MS (ESI) mass spectrum of **2R**. The insets depict the experimental (top) and calculated (bottom) isotopic pattern of the peak.

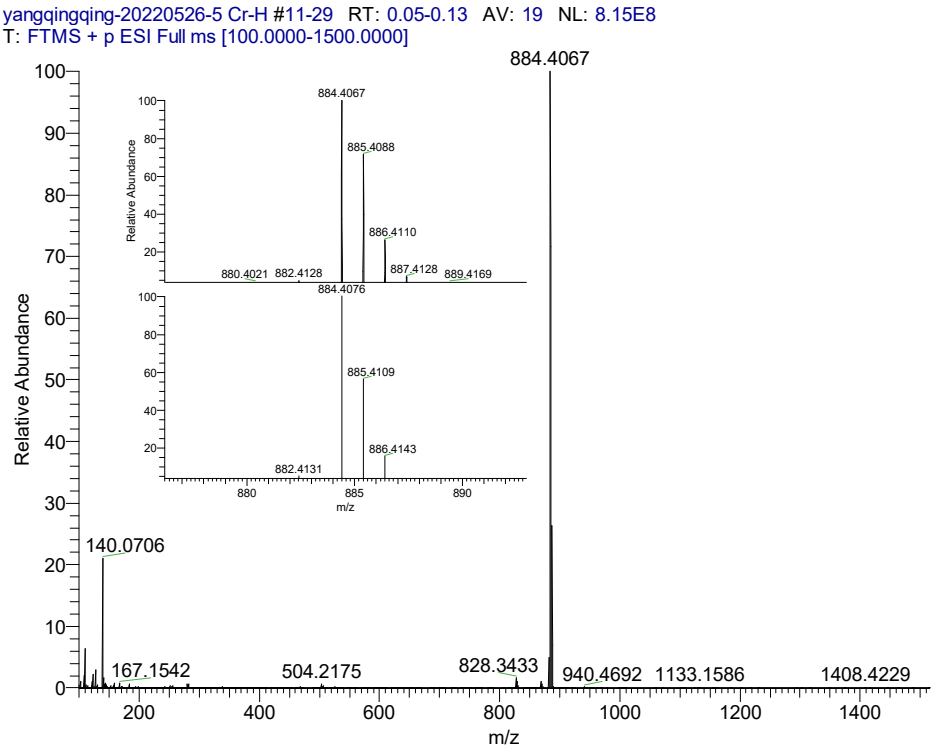


**Figure S15**. HR-MS (ESI) mass spectrum of **3**. The insets depict the experimental (top) and calculated (bottom) isotopic pattern of the peak.

## 5. X-ray crystallography

Single crystals of complexes **1S**, **1R** and **3** for X-ray diffraction studies were obtained by slow diffusion of *n*-hexane into a saturated $CH_2Cl_2$ solution of corresponding Cr complexes. Suitable crystals were selected and detected on a Bruker D8 VENTURE diffractometer. The crystals were kept at 100 K during data collection. Using Olex2[3], the structure was solved with the SHELXT[4] structure solution program using Intrinsic Phasing and refined with the SHELXL[5] refinement package using Least Squares minimisation.

**Table S1**. Crystallographic parameters for the structure of **1S**.

| | |
|---|---|
| Empirical formula | $C_{58}H_{72}Cl_4CrF_6N_6O_4P$ |
| Formula weight | 1255.98 |
| Temperature/K | 100 |
| Crystal system | monoclinic |
| Space group | $P2_1$ |
| *a*/Å | 12.2975(8) |
| *b*/Å | 19.7728(12) |
| c/Å | 12.9875(8) |
| *α*/° | 90 |
| *β*/° | 105.886(2) |
| *γ*/° | 90 |
| Volume/Å$^3$ | 3037.4(3) |
| Z | 2 |
| $\rho_{calc}$/g cm$^{-3}$ | 1.373 |
| $\mu$/mm$^{-1}$ | 0.459 |
| F(000) | 1310.0 |
| Crystal size/mm$^3$ | 0.35 × 0.28 × 0.22 |
| Radiation | MoKα (λ = 0.71073) |
| 2*Θ* range for data collection/° | 4.538 to 61.17 |
| Index ranges | -17 ≤ h ≤ 17, -28 ≤ k ≤ 28, -18 ≤ l ≤ 18 |
| Reflections collected | 66306 |
| Independent reflections | 18607 [$R_{int}$ = 0.0852, $R_{sigma}$ = 0.0835] |
| Data/restraints/parameters | 18607/3/748 |
| Goodness-of-fit on F$^2$ | 1.014 |
| Final *R* indexes [I>=2σ (I)] | $R_1$ = 0.0486, $wR_2$ = 0.1040 |
| Final *R* indexes [all data] | $R_1$ = 0.0782, $wR_2$ = 0.1144 |
| Largest diff. peak/hole / e Å$^{-3}$ | 0.52/-0.58 |
| Flack parameter | -0.023(10) |

**Table S2**. Crystallographic parameters for the structure of **1R**.

| | |
|---|---|
| Empirical formula | $C_{58}H_{72}Cl_4CrF_6N_6O_4P$ |
| Formula weight | 1255.98 |
| Temperature/K | 100 |
| Crystal system | monoclinic |
| Space group | $P2_1$ |
| $a$/Å | 12.2991(5) |
| $b$/Å | 19.7818(8) |
| $c$/Å | 12.9910(5) |
| $\alpha$/° | 90 |
| $\beta$/° | 105.9030(10) |
| $\gamma$/° | 90 |
| Volume/Å$^3$ | 3039.7(2) |
| Z | 2 |
| $\rho_{calc}$/g cm$^{-3}$ | 1.372 |
| $\mu$/mm$^{-1}$ | 0.459 |
| F(000) | 1310.0 |
| Crystal size/mm$^3$ | 0.4 × 0.38 × 0.35 |
| Radiation | MoKα (λ = 0.71073) |
| 2$\Theta$ range for data collection/° | 4.536 to 61.184 |
| Index ranges | -17 ≤ h ≤ 17, -28 ≤ k ≤ 28, -18 ≤ l ≤ 18 |
| Reflections collected | 66954 |
| Independent reflections | 18667 [$R_{int}$ = 0.0431, $R_{sigma}$ = 0.0460] |
| Data/restraints/parameters | 18667/5/747 |
| Goodness-of-fit on F$^2$ | 1.014 |
| Final $R$ indexes [I>=2σ (I)] | $R_1$ = 0.0401, $wR_2$ = 0.0891 |
| Final $R$ indexes [all data] | $R_1$ = 0.0541, $wR_2$ = 0.0957 |
| Largest diff. peak/hole / e Å$^{-3}$ | 0.61/-0.54 |
| Flack parameter | -0.010(5) |

**Table S3**. Crystallographic parameters for the structure of **3**.

| | |
|---|---|
| Empirical formula | $C_{53}H_{62}Cl_2CrF_6N_6O_4P$ |
| Formula weight | 1114.95 |
| Temperature/K | 100.0(2) |
| Crystal system | monoclinic |
| Space group | *C*2/*c* |
| *a*/Å | 27.3793(15) |
| *b*/Å | 19.1458(10) |
| *c*/Å | 21.6094(11) |
| $\alpha$/° | 90 |
| $\beta$/° | 114.666(3) |
| $\gamma$/° | 90 |
| Volume/Å$^3$ | 10294.0(10) |
| Z | 8 |
| $\rho_{calc}$/g cm$^{-3}$ | 1.439 |
| $\mu$/mm$^{-1}$ | 3.708 |
| F(000) | 4648.0 |
| Crystal size/mm$^3$ | 0.24 × 0.22 × 0.19 |
| Radiation | CuKα (λ = 1.54178) |
| 2$\Theta$ range for data collection/° | 5.824 to 136.756 |
| Index ranges | -32 ≤ h ≤ 32, -23 ≤ k ≤ 23, -25 ≤ l ≤ 26 |
| Reflections collected | 75165 |
| Independent reflections | 9400 [$R_{int}$ = 0.0927, $R_{sigma}$ = 0.0437] |
| Data/restraints/parameters | 9400/167/734 |
| Goodness-of-fit on F$^2$ | 1.023 |
| Final *R* indexes [I>=2σ (I)] | $R_1$ = 0.0494, $wR_2$ = 0.1258 |
| Final *R* indexes [all data] | $R_1$ = 0.0581, $wR_2$ = 0.1340 |
| Largest diff. peak/hole / e Å$^{-3}$ | 0.83/-0.52 |

**Table S4.** Selected bond lengths and bond angles obtained from crystallographic data for complexes **1S, 1R** and **3**.

| Complex | | **1S** | **1R** | **3** |
|---|---|---|---|---|
| Bond Angles (°) | N(amido)-Cr-N(amido) | 179.33(12) | 179.27(10) | 178.58(9) |
| | N(oxazoline)-Cr-N(oxazoline) | 176.55(11) | 176.34(9) | 175.19(9) |
| | | 176.29(11) | 176.59(9) | 174.87(9) |
| Bond Lengths (Å) | Cr-N(amido) | 1.988(3) | 1.988(2) | 1.994(2) |
| | | 1.990(3) | 1.989(2) | 1.999(2) |
| | Cr-N(oxazoline) | 2.074(2) | 2.081(2) | 2.059(2) |
| | | 2.068(2) | 2.086(2) | 2.069(2) |
| | | 2.084(3) | 2.074(2) | 2.040(2) |
| | | 2.078(3) | 2.069(2) | 2.059(2) |

**6.** Excited State Properties

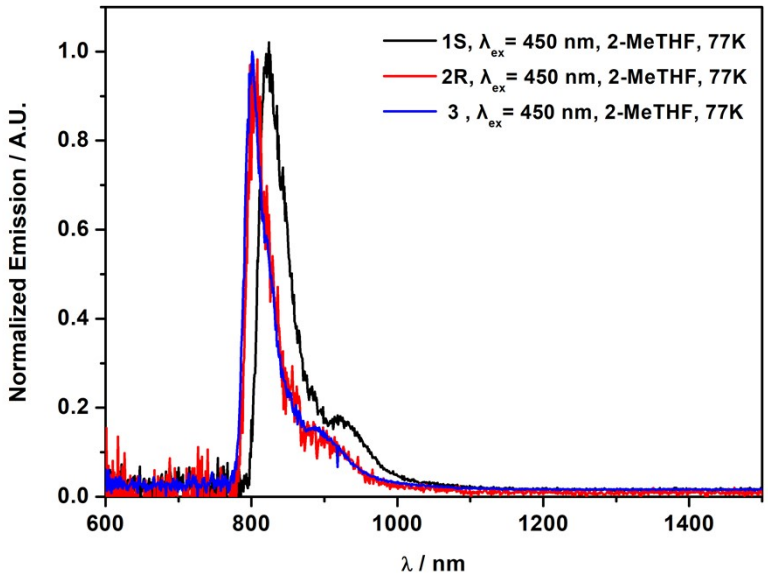


**Figure S16**. Emission spectra of **1**–**3** in 2-methyltetrahydrofuran at 77K (concentration $1\times10^{-5}$ M).

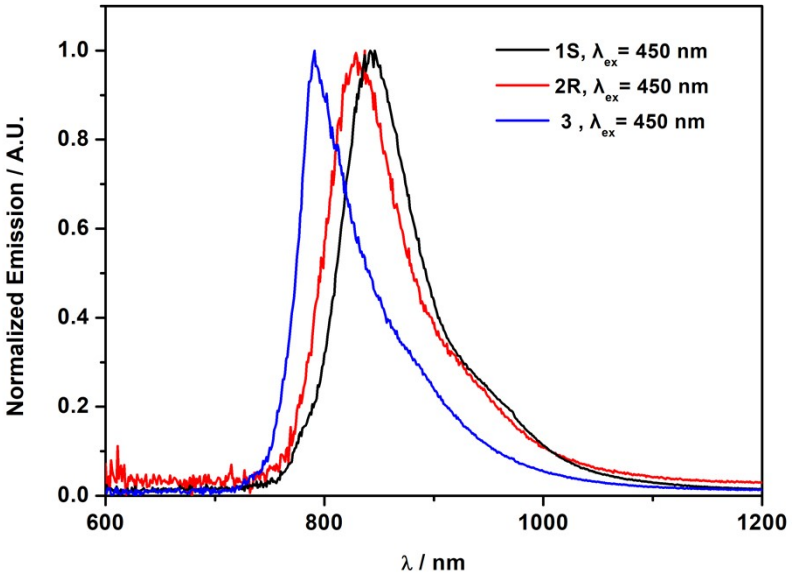


**Figure S17**. Emission spectra of **1**–**3** in the solid state at room temperature.

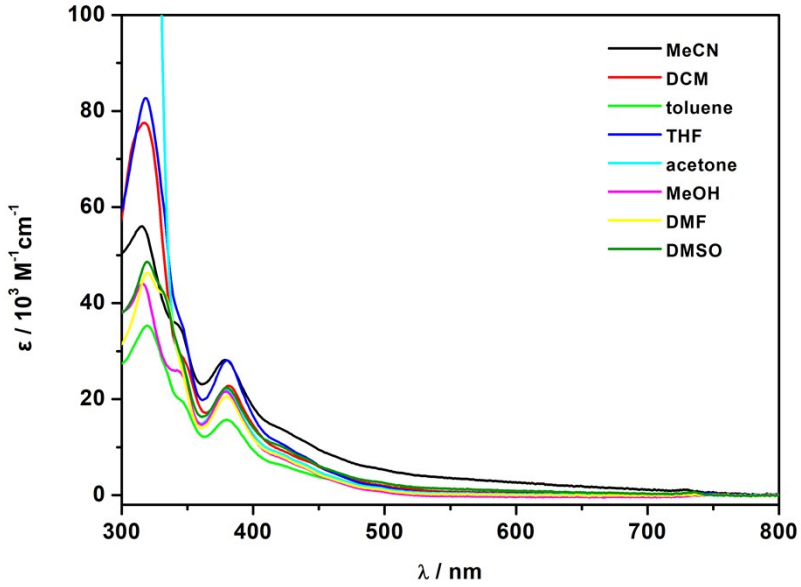


**Figure S18**. UV-vis absorption spectra of complex **1S** in different solvents (concentration $1\times10^{-5}$ M).

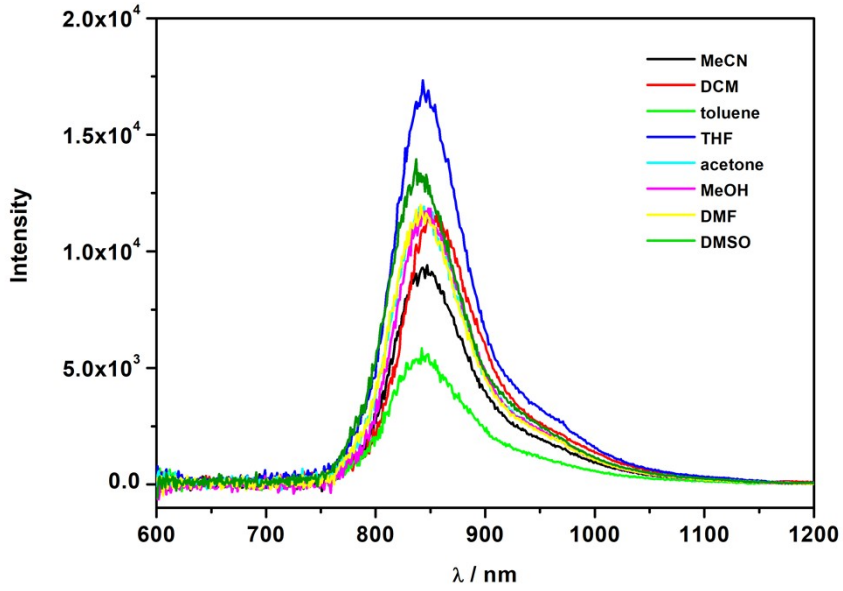


**Figure S19**. Emission spectra of complex **1S** in different solvents (concentration $1\times10^{-5}$ M) at 298 K upon excitation at 450 nm.

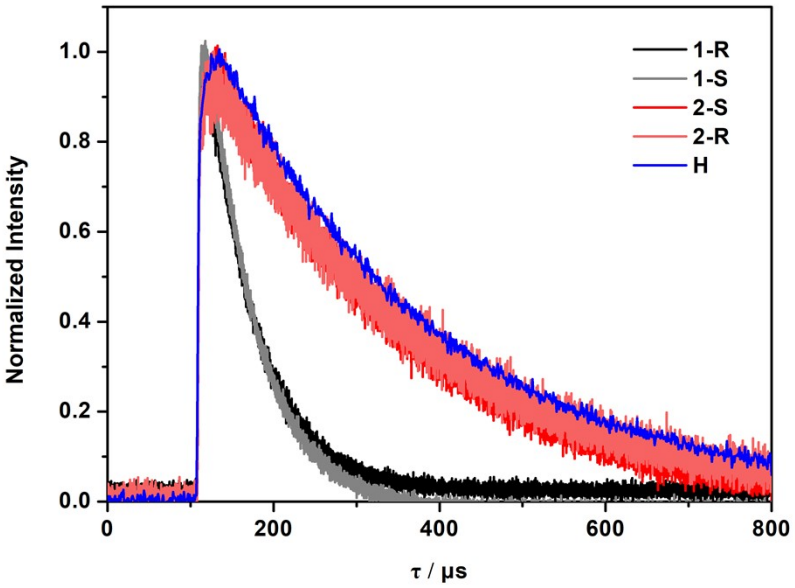


**Figure S20**. Phosphorescence decay curves of complexes **1S**/**1R**, **2S**/**2R** and **3** in degassed MeCN (concentration $1 \times 10^{-5}$ M) at 298 K upon excitation at 450 nm.

**Table S5**. Lifetime of complexes **1**–**3** in different solvents (concentration $1\times10^{-5}$ M) upon excitation at 450 nm.

| Complex | Condition | $\lambda_{em}$ / nm | τ / μs | Φ |
|---|---|---|---|---|
| **1R** | 2-MeTHF, 77K | 820, 925 | 433.63, 407.68 | |
| | Degassed MeCN, rt. | 845 | 56.58 | 0.024 |
| | MeCN, rt. | 845 | 23.69 | |
| **1S** | 2-MeTHF, 77K | 820, 925 | 435.50, 425.13 | |
| | Degassed MeCN, rt. | 845 | 57.39 | 0.025 |
| | MeCN, rt. | 845 | 23.69 | |
| | Solid, rt. | 842 | 15.84 | 0.010 |
| **2R** | 2-MeTHF, 77K | 805, 905 | 463.90, 436.87 | |
| | Degassed MeCN, rt. | 820 | 259.37 | 0.066 |
| | MeCN, rt. | 820 | 10.03 | |
| | Solid, rt. | 830 | 74.78 | 0.037 |
| **2S** | 2-MeTHF, 77K | 805, 905 | 465.21, 441.57 | |
| | Degassed MeCN, rt. | 820 | 247.53 | 0.075 |
| | MeCN, rt. | 820 | 10.66 | |
| **3** | 2-MeTHF, 77K | 801, 890 | 490.07, 492.37 | |
| | Degassed MeCN, rt. | 813 | 266.70 | 0.082 |
| | MeCN, rt. | 813 | 14.14 | |
| | Solid, rt. | 790 | 104.62 | 0.066 |

**7.** Electronic circular dichroism and circularly polarized luminescence

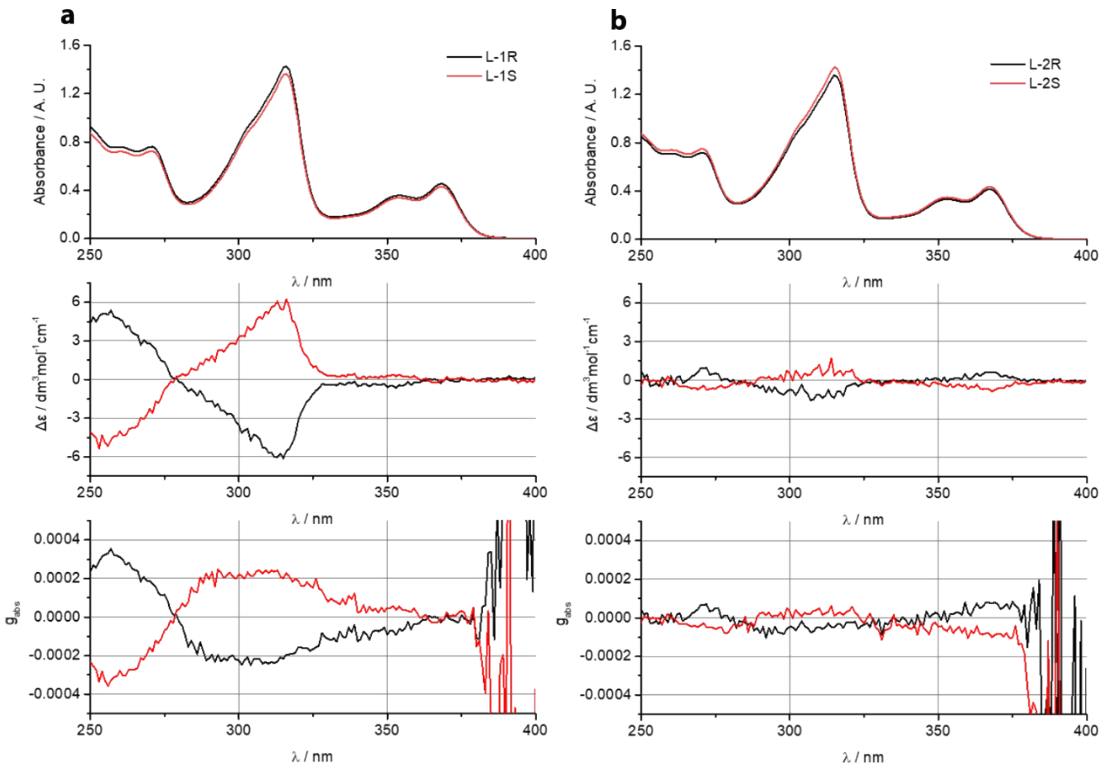


**Figure S21**. Absorption spectra, electronic circular dichroism and plots of absorption dissymmetry factor $g_{abs}$ of the ligands (a) **L-1S**, **L-1R** and (b) **L-2S**, **L-2R** in deaerated MeCN (concentration $5 \times 10^{-5}$ M) at 298 K.

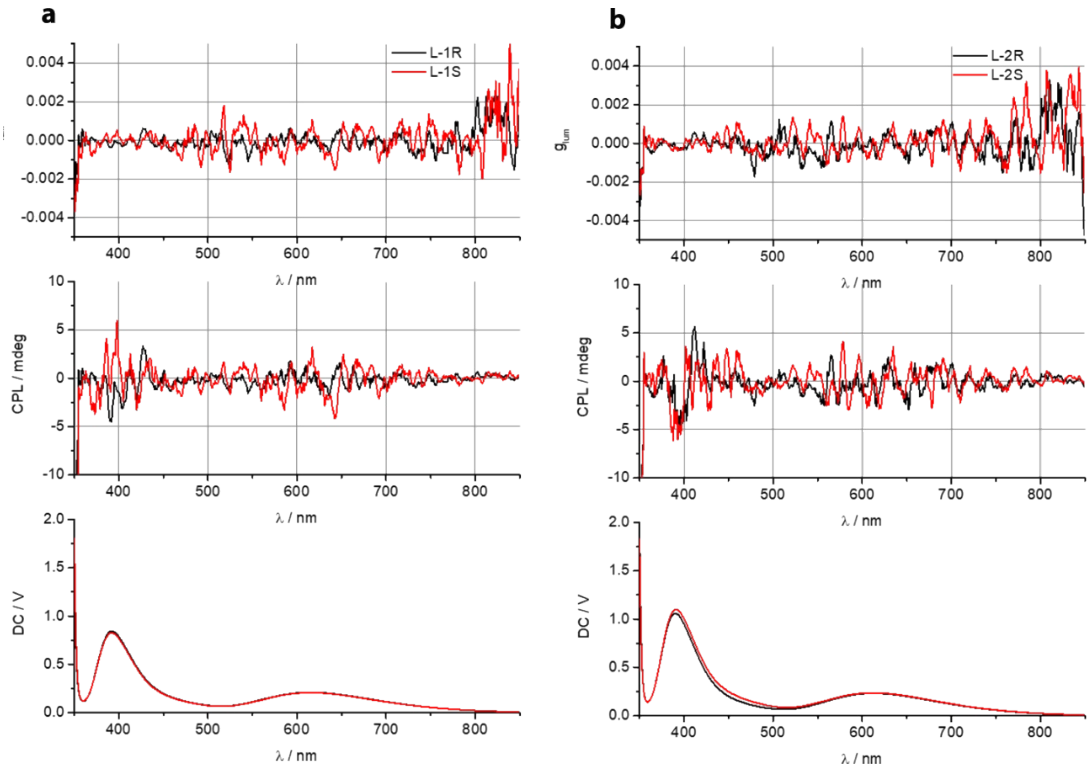


**Figure S22**. Plots of luminescence dissymmetry factor $g_{lum}$, CPL degree and DC signal for (a) **L-1S**, **L-1R** and (b) **L-2S**, **L-2R** in deaerated MeCN (concentration $5 \times 10^{-5}$ M) at 298 K.

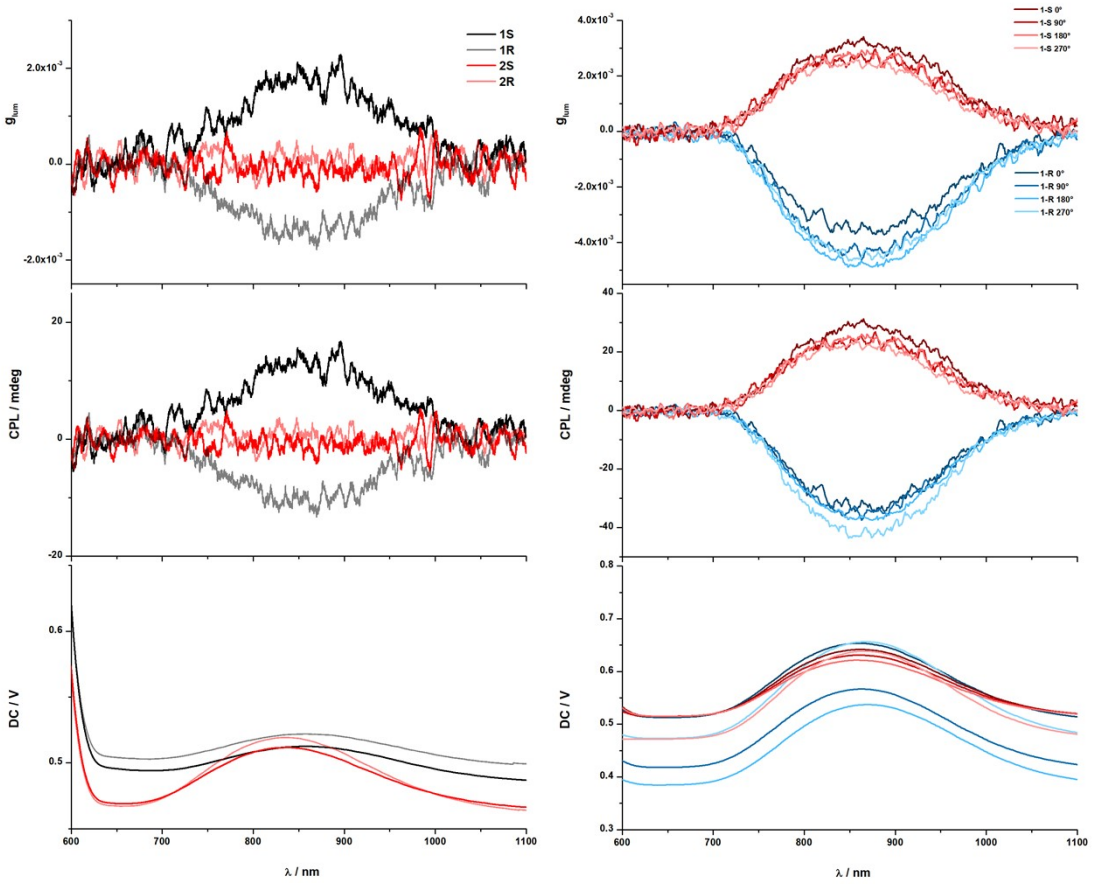


**Figure S23**. Plots of luminescence dissymmetry factor $g_{lum}$, CPL degree and DC signal for **1S/1R** and **2S/2R** in deaerated MeCN at 298 K (left) and **1S/1R** in the solid state at 298 K (right).

**8.** X-ray photoelectron spectroscopy (XPS) and ultraviolet photoelectron spectroscopy (UPS)

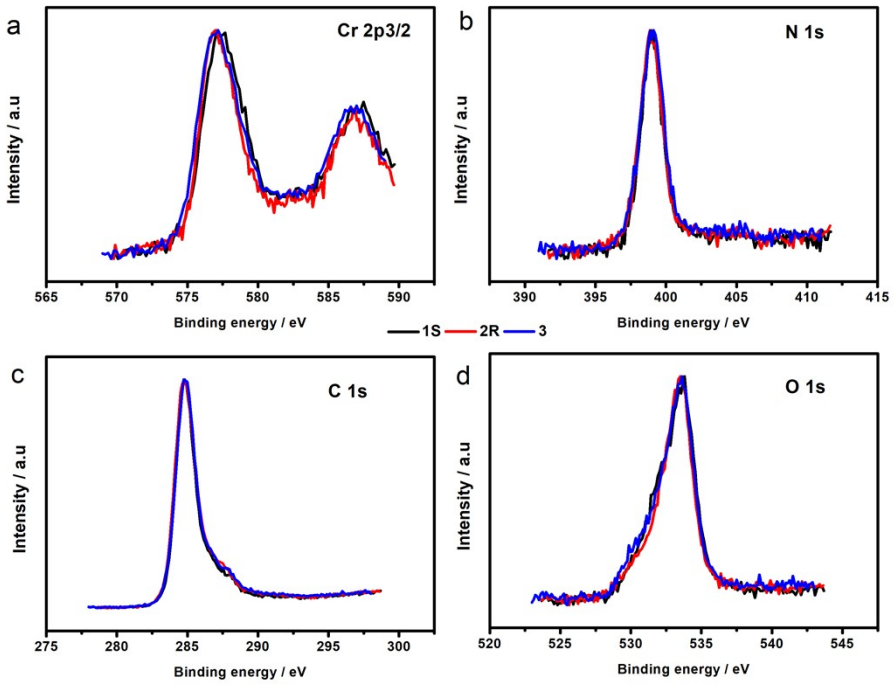


**Figure S24**. XPS spectra of complexes **1**–**3** films: (a) Cr 2p 3/2 (b) N 1s (c) C 1s (d) O 1s.

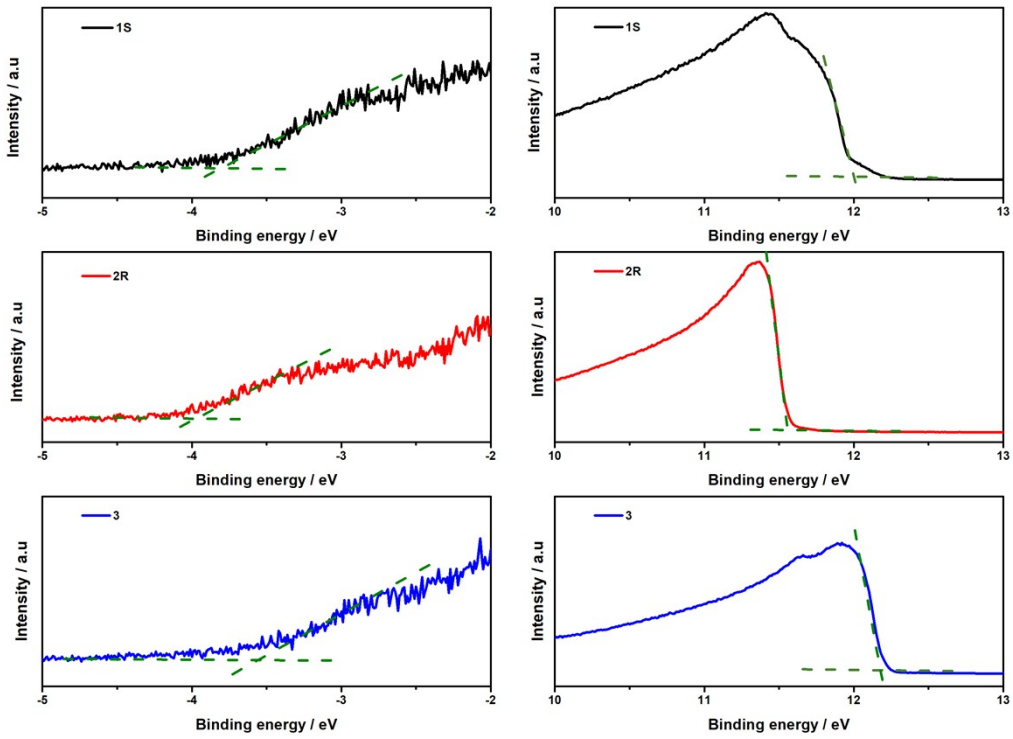


**Figure S25**. UPS spectra of complexes **1**–**3** films (left: valence region cutoff; right: secondary electron cutoff).

The HOMO energies of **1**–**3** were measured using UPS measurements.[6] The abscissa is the binding energy relative to the Fermi energy ($E_F$) of Cr, which is defined by the energy of the electron before excitation relative to the vacuum level. Fig. S23 shows the high binding energy cutoff ($E_{cutoff}$) of the **1**–**3** thin film; $E_{cutoff}$ is determined by linear extrapolation to zero of the yield of secondary electrons. The $E_{onset}$ is the onset of the **1**–**3** thin film relative the Fermi energy ($E_F$) of Cr. Their HOMO energies were then calculated using the following equation:

$$E_{HOMO} = h\nu - (E_{cutoff} - E_{onset})$$

where $h\nu$ = 21.22 eV is the incident photo energy value of the He(I) source.

## 9. Electrochemical property

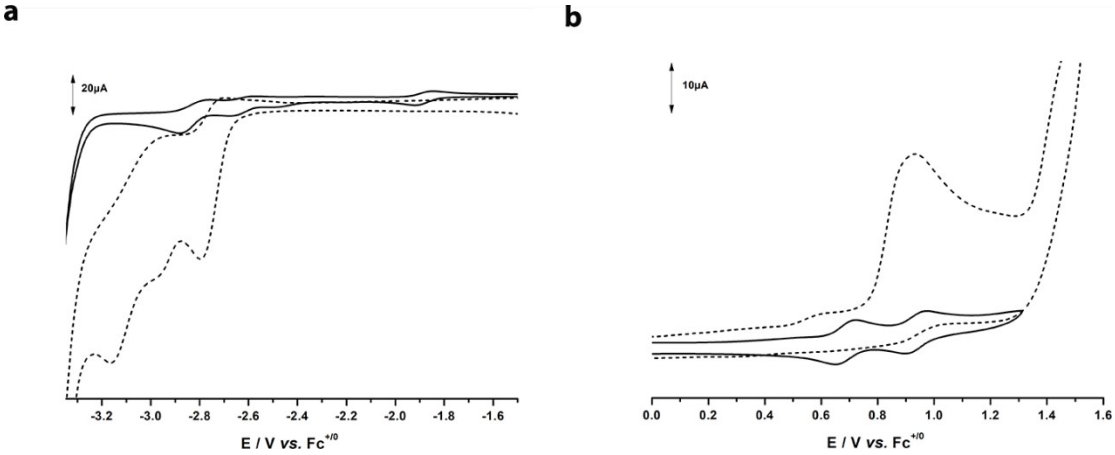


**Figure S26.** Cyclic voltammogram of 1 mM **1S** (full line) and 1mM ligand **L1** (dotted line) in MeCN with 0.1 M of $^{n}Bu_4NPF_6$ as supporting electrolyte, recorded at a scan rate of 0.1 V/s.

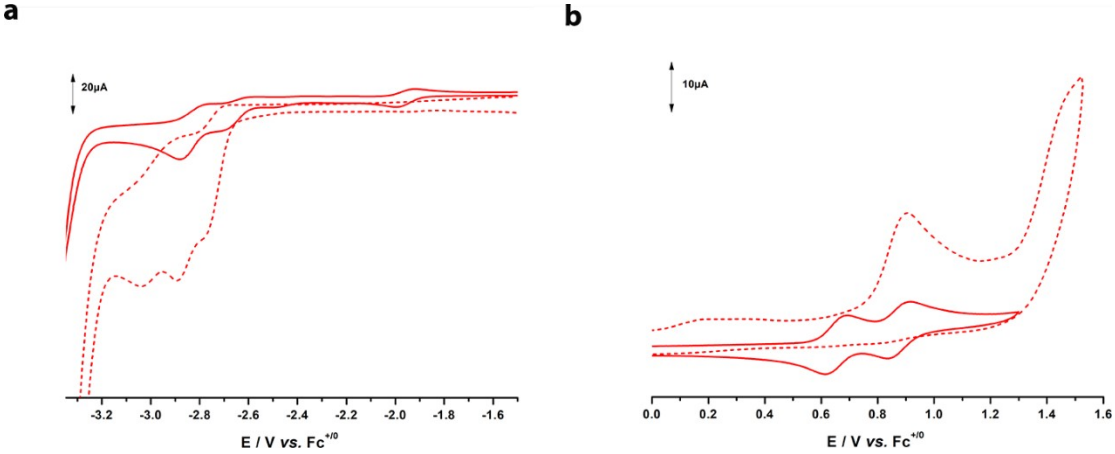


**Figure S27.** Cyclic voltammogram of 1 mM **2S** (full line) and 1mM ligand **L3** (dotted line) in MeCN with 0.1 M of $^{n}Bu_4NPF_6$ as supporting electrolyte, recorded at a scan rate of 0.1 V/s.

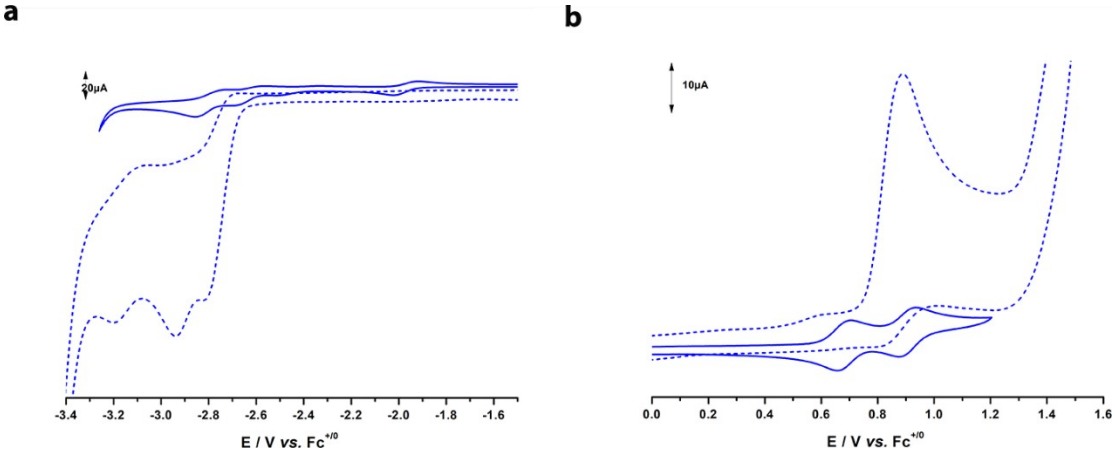


**Figure S28.** Cyclic voltammogram of 1 mM **3** (full line) and 1mM ligand **L3** (dotted line)

in MeCN with 0.1 M of $^{n}Bu_4NPF_6$ as supporting electrolyte, recorded at a scan rate of 0.1 V/s.

**Table S6.** Electrochemical potentials ($E_{1/2}$ in V vs $Fc^{+/0}$) of **1**–**3**.

| Compound | $E_{1/2}(Cr^{IV/III})$ | $E_{1/2}((L^{\bullet+/0})$ | $E_{1/2}(Cr^{II/III})$ | $E_{1/2}(L^{0/\bullet-})$ |
|---|---|---|---|---|
| **1S** | 0.76 | 1.00 | –1.90 | –2.47 |
| **2S** | 0.68 | 0.90 | –2.00 | –2.47 |
| **3** | 0.70 | 0.93 | –2.00 | –2.48 |
| $[Cr(dpc)]^{+}$ | 0.46 | 0.78 | –1.51 | –2.45 |

**10.** Transient absorption (TA) spectroscopy

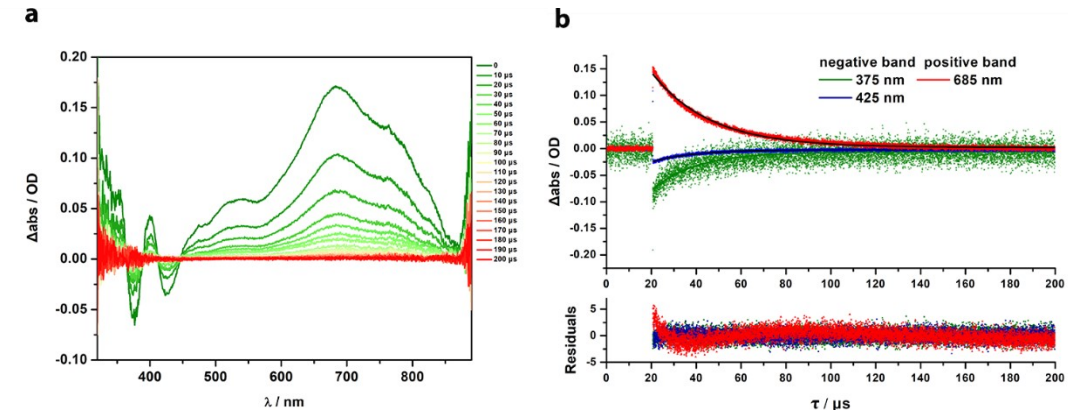


**Figure S29**. Time-resolved TA spectra (a) and kinetic decays (b) of **1R** ($1\times10^{-4}$ M in deaerated MeCN) recorded at 298 K excited with 355 nm pump laser pulses.

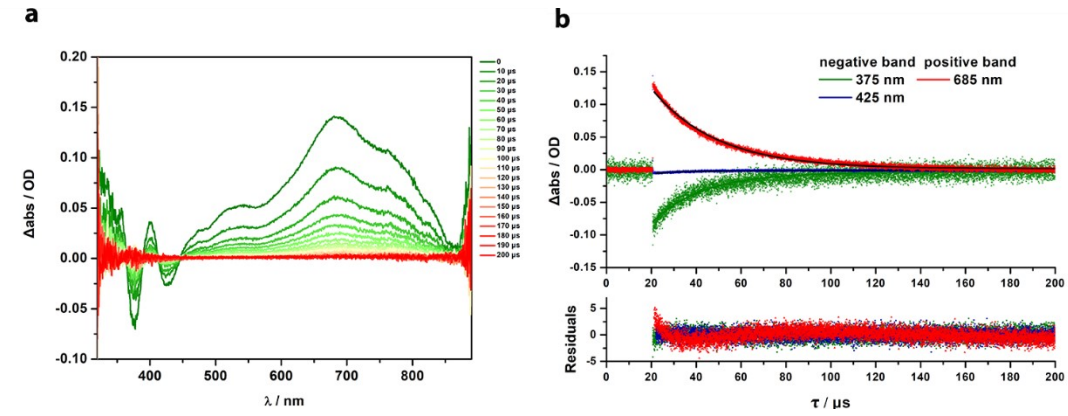


**Figure S30**. Time-resolved TA spectra (a) and kinetic decays (b) of **1S** ($1\times10^{-4}$ M in deaerated MeCN) recorded at 298 K excited with 355 nm pump laser pulses.

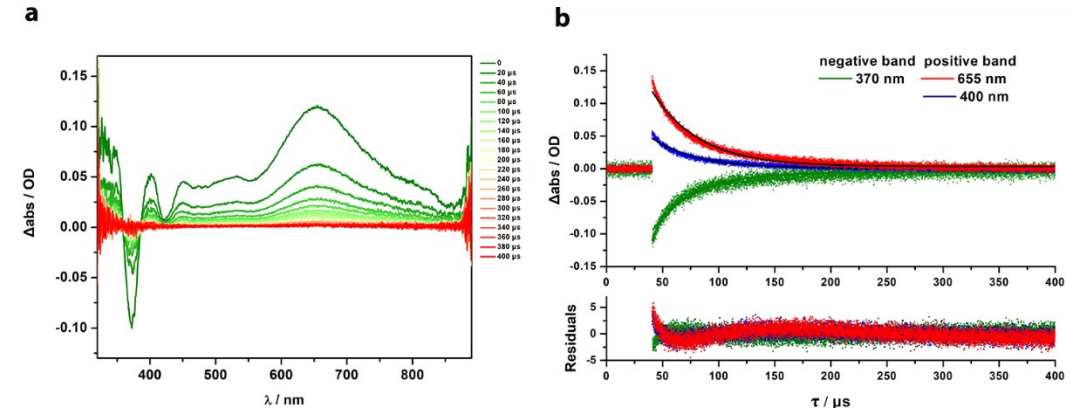


**Figure S31**. Time-resolved TA spectra (a) and kinetic decays (b) of **2R** ($1\times10^{-4}$ M in deaerated MeCN) recorded at 298 K excited with 355 nm pump laser pulses.

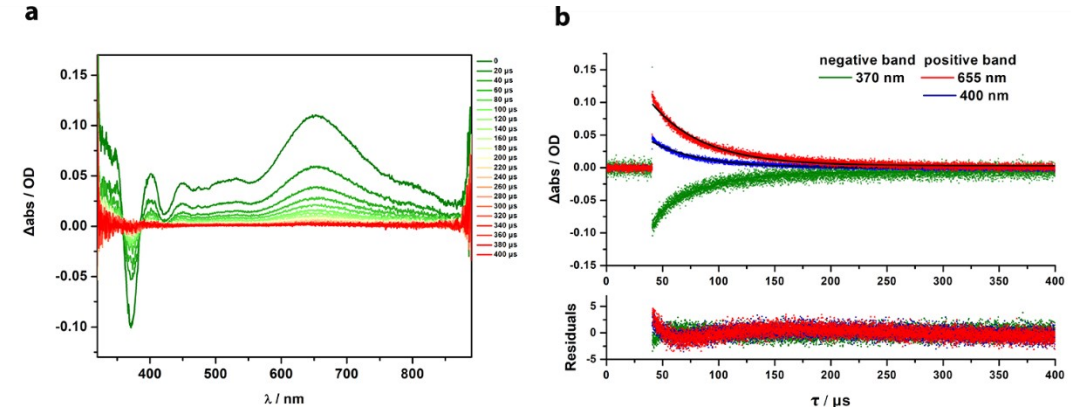


**Figure S32**. Time-resolved TA spectra (a) and kinetic decays (b) of **2S** ($1\times10^{-4}$ M in deaerated MeCN) recorded at 298 K excited with 355 nm pump laser pulses.

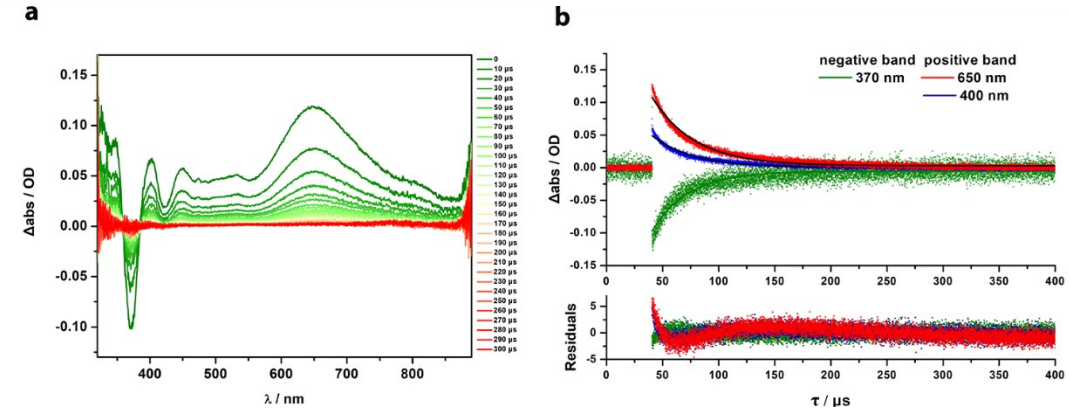


**Figure S33**. Time-resolved TA spectra (a) and kinetic decays (b) of **3** ($1\times10^{-4}$ M in deaerated MeCN) recorded at 298 K excited with 355 nm pump laser pulses.

**Table S7** The decaying components of **1**–**3** ($1\times10^{-4}$ M in deaerated MeCN) relating to the transient absorption at 298 K excited with 355 nm pump laser pulses.

| **Complex** | **τ at 298 K / μs** | | |
|---|---|---|---|
| **1R** | 19.52 (375 nm) | 18.52 (425 nm) | 26.01 (685 nm) |
| **1S** | 22.93 (375 nm) | 17.16 (425 nm) | 28.93 (685 nm) |
| **2R** | 41.85 (370 nm) | 44.01 (400 nm) | 46.89 (655 nm) |
| **2S** | 37.45 (370 nm) | 40.46 (400 nm) | 41.87 (655 nm) |
| **3** | 31.98 (370 nm) | 36.03 (400 nm) | 37.84 (650 nm) |

**11.** Spectro-electrochemistry

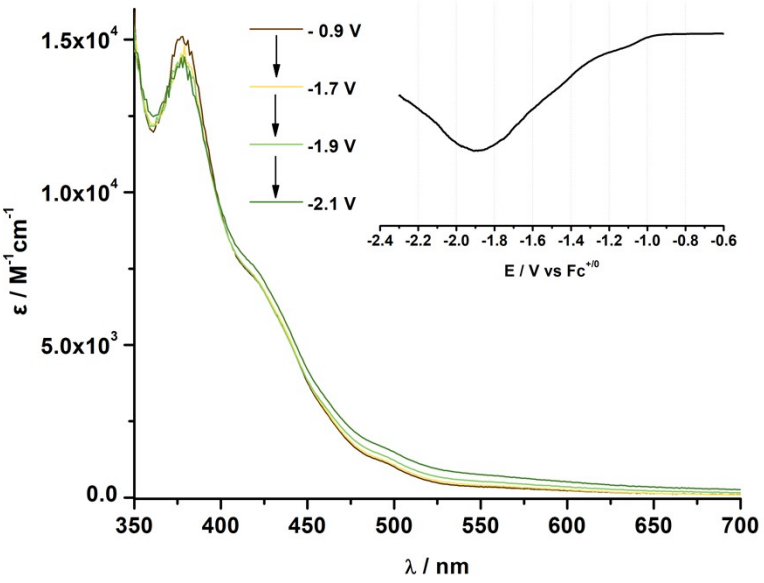


**Figure S34**. Spectro-electrochemistry of **1S** ($1\times10^{-4}$ M in MeCN) with applied potentials in the electrochemical cell.

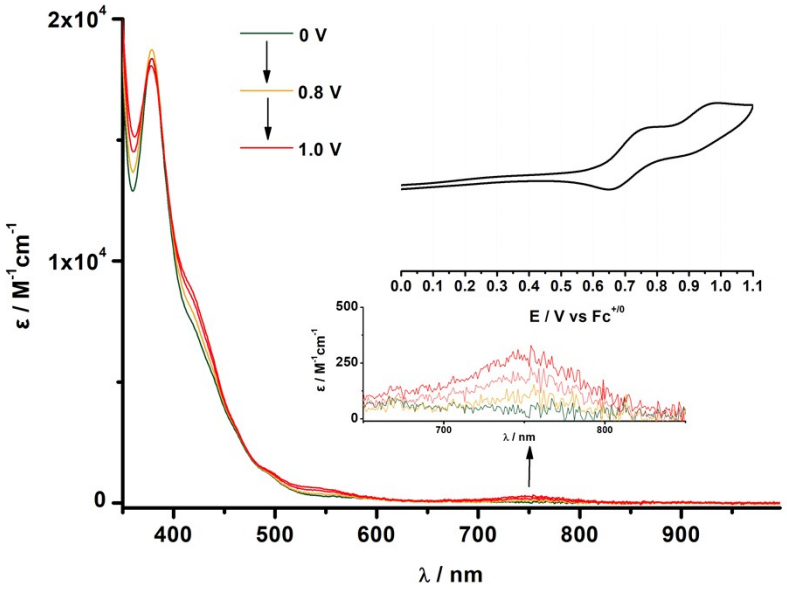


**Figure S35**. Spectro-electrochemistry of **1S** ($1\times10^{-4}$ M in MeCN) with applied potentials in the electrochemical cell.

**[References]**


1. N. Sinha, J.-R. Jiménez, B. Pfund, A. Prescimone, C. Piguet and O. S. Wenger, *Angew. Chem. Int. Ed.*, 2021, **60**, 23722-23728.
2. M. Durán-Galván, S. A. Worlikar and B. T. Connell, *Tetrahedron*, 2010, **66**, 7707-7719.
3. O. V. Dolomanov, L. J. Bourhis, R. J. Gildea, J. A. K. Howard and H. Puschmann, *J. Appl. Crystallogr.*, 2009, **42**, 339-341.
4. G. Sheldrick, *Acta Crystallogr. A*, 2015, **71**, 3-8.
5. G. Sheldrick, *Acta Crystallogr. C*, 2015, **71**, 3-8.
6. L. Zheng, T. Zhu, W. Xu, L. Liu, J. Zheng, X. Gong and F. Wudl, *J. Mater. Chem. C*, 2018, **6**, 3634-3641.